Egypt. J. Bot. **Vol. 63**, No. 3, pp. 1201-1214 (2023)

Egyptian Journal of Botany
http://ejbo.journals.ekb.eg/

Antibiofilm Activity of Biosynt h esized Enterococcus-Iron Oxide Nanoparticles against Uropathogenic Bacteria

Mohammed A. Ali[#], Marwa H. Alkhafaji
Department of Biology, College of Science, Baghdad University, Baghdad, Iraq.

THE PATHOGENICITY of the bacteria is significantly influenced by the virulence factors, such as biofilm. Urinary tract infections (UTIs), a common urologic condition that affects millions of individuals worldwide, are caused by bacteria that are extremely resistant to antimicrobials. Therefore, the goal of this work was to use nanoparticles as contemporary antimicrobials to discover a solution to this worldwide issue. For the first time, *Enterococcus faecalis* isolates from food sources were used to naturally create iron oxide nanoparticles (E-IONPs). The biosynthesis process was done in optimized conditions at 1M of concentration of iron oxide solution at 60 ˚C for the incubation period of 24h at pH 5. The bacterial isolates were isolated from clinical and food samples. After being identified, food-origin bacteria were used in the biosynthesis process, while the clinical isolates were evaluated for their ability to form biofilm. E-IONPs were firstly characterized by color change, then by UV-vis spectroscopy, AFM, FTIR, and SEM analysis. The anti-biofilm activity of the super-magnetic E-IONPs was assessed using a microtiter plate assay. Our results revealed that the biosynthesized E-IONPs were cubic and irregular in shape, and they have an anti-biofilm activity against *Escherichia coli*, *Staphylococcus aureus*, *Klebsiella pneumonia*, and *Streptococcus agalactiae*. Eventually, the biosynthesized super-magnetic iron oxide nanoparticles were concluded to be effective against biofilm formed by uropathogenic bacteria.

Keywords: Biofilms, *Enterococcus faecalis*, Super-magnetic iron oxide nanoparticles, UTI, Virulence.

Introduction

Most hospital admissions throughout the world are due to urinary tract infections (UTIs), which are a severe health issue and have comorbidities in patients with underlying conditions. In those without anatomical or functional problems, UTIs typically go away on their own, although they tend to come back (Odoki et al., 2019). Although many microbes can invade the urinary tract and causing infection, Gram-positive and Gram-negative bacteria, as well as some fungi, are the most common causes of UTIs. The most frequent causes of both mild and severe urinary tract infections are uropathogenic *E. coli* and *S. aureus* (Priya, 2019). Antimicrobial resistance is a grave issue that requires immediate attention (Galindo-Méndez, 2020). Most bacteria exhibit a significant antibiotic resistance, which is a grave issue. The most typical organisms that cause resistance to antibiotics are *S. aureus* and *E. coli* (Wu et al., 2021; Larsen et al., 2022). Due to widespread *E. coli* fluoroquinolone medication resistance, urinary tract infections (UTIs), which are 90–80% of the time caused by *E. coli*, cannot be treated (Kumar et al., 2022). *S. aureus*, a gram-positive pathogenic agent and one of the bacteria causing the sickness, can enter the urinary system. Although the illness is a recently reported cause in urinary tract infections (UTI), accounting for 1% of simple cases and 3% of complex cases, it can become life-threatening if left untreated (Paudel et al., 2021). It has to do with the urinary system being physically blocked. A biofilm shields bacteria from drugs (Singh et al., 2021). A surge in morbidity and death from microbial infections has been related to the prevalence of multidrug-resistant bacteria. A factor contributing to the rise in multidrug resistance is the dearth of innovative and potent

[#]Corresponding author email: mhamadali550.ma@gmail.com Mobile phone number: 009647713328335
Received 22/08/2022; Accepted 30/10/2022
DOI: 10.21608/ejbo.2022.157735.2111
Edited by: Dr. Hamdy Zahran, National Research Centre, 12622 Dokki, Cairo, Egypt

antibiotics. Antimicrobial nanoparticles (NPs) have been spotlighted recently (Mba & Nweze, 2021). For example, IONPs have shown an immense potential in biomedicine, agriculture, cosmetics, bioremediation, diagnostics, and engineering materials (Huh & Kwon, 2011; Nadeem et al., 2021). Iron oxides in nature include antiferromagnetic hematite (α-Fe_2O_3), paramagnetic maghemite (γ-Fe_2O_3), and supermagnetic magnetite (Fe_3O_4) (Sampora et al., 2022). Fe_3O_4 NPs exhibit a minimal toxicity, biocompatibility, cost-effectiveness, and a high surface area to volume ratio compared to the other nanoparticles (Yazdanian et al., 2022). Nanoparticles may be produced using a wide range of techniques. Most of the time, chemical or physical processes may be used to create nanoparticles (Sohal et al., 2021). As a result, this approach may be pricey and harmful to the environment. In response to these issues, the synthetic process known as a biosynthesis was developed. Since it is affordable, simple, straightforward, and non-toxic, the biosynthesis of nanoparticles using microbes is developing as an environmentally acceptable technique. Bacterial nanoparticles must constantly have their size and form under control (Youssef et al., 2019: Ojo et al., 2021). To eliminate the biofilm-forming bacteria that repeatedly cause urinary tract infections, this study sought to biosynthesize iron oxide nanoparticles from food-sourced *E. faecalis*.

Materials and Methods

Isolation of bacteria

Sixty random food samples (dairy milk, vegetables, meat, and fish) were collected from Baghdad markets between September and November 2021. Samples were inoculated on bile esculin agar plates and incubated for 24h at 37°C. When bile is present, *Enterococci* and group D *Streptococci* hydrolyze esculin (Swan, 1954: Yerlikaya & Akbulut, 2020). A 100-urine specimen was collected from the patients with urinary tract infections. The samples were then cultured on selective culture media and aerobically incubated at 37°C for 24h.

Identification of the isolates

All the isolated bacteria were identified using the colonial morphology on selective and differential culture media (Benson, 2001; Mao et al., 2020). Meanwhile, the VITEK2 system was utilized to verify the results.

Biofilm formation assay

The gold standard method for biofilm detection is the microtiter plate method to conduct a quantitative test method for the biofilm detection (Jogi et al., 2022). This is the gold standard one. Isolates *of S. aureus, E. coli, K. pneumoniae,* and *S. agalactiae* were inoculated in 10mL of trypticase soy broth (TSB) containing 1% glucose w/v and incubated for 24h at 37°C. A new medium was used to dilute the culture to reach a final concentration of 1:100, and the wells were subsequently filled with the sterile broth as a negative control. Afterwards, the plates were incubated for 24h at 37°C, and the contents of each well were gently tapped to remove them from the plates. After a triple wash with a sterile distilled water, the wells were free of planktonic bacteria. The biofilm formed in the wells was stained with a crystal violet (0.1%, w/v). This solution was prepared by dissolving 0.1g of crystal violet stain in 100mL of D.W (Grassi et al., 2019). The plates were allowed to dry. The stained biofilm was then detected by Micro ELISA auto reader model 680 (Biorad, UK) at 630 nm and its optical density (OD) was recorded. The results were conducted according to Table 1 (Manandhar et al., 2018).

TABLE 1. Clarification of the biofilm production

Average OD value	Biofilm production
≤ OD /ODc < ~ ≤ 2x ODc	Non / weak
2x ODc < ~ ≤ 4 x ODc	Moderate
> 4x ODc	Strong

*ODc: Optical density of control negative.

Steps biosynthesis of Iron oxide nanoparticles

Preparation of the bacterial filtrate of E. faecalis

A fresh culture of food origin *E. faecalis* was cultured on a nutrient broth for 18h at 37°C. The tubes were then centrifuged for 10min at 10,000rpm to collect the bacterial supernatant.

Preparation stock solution of IO salt (FeCl-.6H-O)

For the stock solution preparation in 1M, a 27 g of FeCl-.6H-O was dissolved in 100mL deionized distilled water (D.D.W).

Biosynthesis of iron nanoparticles (Fe-O-NPs)

With certain changes for this work, the method for the biosynthesis of IONPs follows the reports of Hassan & Mahmood (2019) and Üstün et al. (2022). A 1mL of *E. faecalis* filtrate was mixed to 3mL of 1M FeCl-.6H-O at 60°C to biosynthesize the iron nanoparticles. The colour eventually transitioned from yellowish brown to pale yellow and then, after many hours, to brownish black. The shift in hue denotes the creation of iron nanoparticles (Fe_3O_4) and the reduction of Fe^{+3} to Fe^{+4} as portrayed in Fig 1.

Optimization of the conditions for E-IONPs biosynthesis

Many factors, including pH, temperature, incubation durations, and the biosynthesis reaction mixture, were evaluated to determine whether they could improve the nanoparticles' quality or not.

Incubation period and temperature

The incubation at different temperatures (4, 25, and 37°C) for different times (24, 48, and 72h) was applied. A culture supernatant free of iron was kept as a negative control. After that, the formed iron oxide nanoparticles were analyzed.

pH-optimization

The pH value of the reaction mixture was assessed at different values (5, 7, and 14). After the incubation period, the iron oxide nanoparticles were analyzed.

Reaction mixture optimization

The proportions of reaction precursors, including bacterial supernatant and iron oxide salt were 1:1, 1:3, 2:6, and 1:9. Two controls, one for bacterial supernatant and the second for iron oxide salt, were then kept. The resulted iron oxide nanoparticles were characterized.

Characterization of Iron oxide nanoparticles

UV-Vis's spectra

The E-IONPs were assessed in a 2mL quartz cuvette with a 1cm path length by measuring the wavelength of the reaction mixture in the UV-Vis spectrum with a resolution of 1 nm. With a range of 300-900nm, the samples were scanned at 500nm min^{-1}. The spectrophotometer was calibrated using a blank reference. The UV-Vis absorption spectra of all samples were recorded and visualized (Hashim & AlKhafaji, 2018).

Scanning electron microscope

A scanning electron microscope (SEM) was used to determine the average shape of nanoparticles. After being sonicated; it was suspended with D.D.W., and a drop of E-IONPs solution was deposited on a glass slide and left to dry. They were plated with a platinum to make them conductors (Nixon, 2008: Shi et al., 2020).

Atomic force microscopy

The E-IONPs were studied using atomic force microscopy. On the silica glass slide, a thin film of E-IONPs was dropped onto the surface. AFM was used to scan the film that had been deposited to detect the average size, granularity, and diameter of nanoparticles.

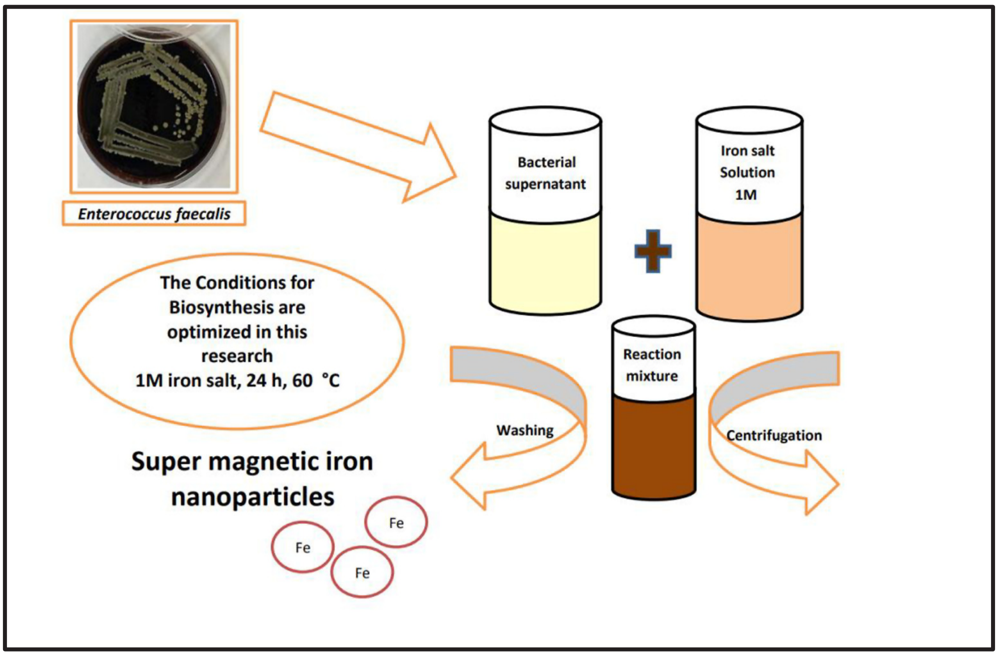

Fig. 1. Schematic view for the biosynthesis process of *Enterococcus*-Iron oxide nanoparticles

Fourier transform infrared spectroscopy

FTIR in the range of 4000-450cm^{-1} at a resolution of 4cm^{-1} was used to suppose the potential interaction between the nanoparticle surface and the mixed bacterial supernatant.

Evaluation of the antibiofilm activity of Iron oxide nanoparticle

The method outlined by Shkodenko et al. (2020) used a 96-well microtiter plate that was inoculated with the overnight culture of *E. coli*, *K. pneumoniae*, *S. aureus*, and *S. agalaciae* which were grown in TSB-glucose (TSB + 1% w/v glucose). The isolates were diluted to 1:100 (100mL of Meuller Hinton broth) in the wells. Each well of the microtiter plate was loaded with 100µL of the inoculated medium and 100µL of E-IONPs. The control positive was IONP-free bacterial culture, while the negative control was the mere broth. For the next 24h, the plate was kept at 37°C. Then 0.1% w/v of crystal violet solution was used to stain the plate for 10min at room temperature. After that the stain was removed by submerging the plate in a water-filled tray. Microtiter plates were placed on paper towels and allowed to dry to eliminate excess moisture. Treatment with 33% v/v of glacial acetic acid for 15min at room temperature was applied on the stained wells to solubilize the dye. We checked the optical density of the stained wells by ELISA auto reader at 630nm.

Statistical analysis

One-way ANOVA was utilized in a factorial experiment with a completely random design. The least significant difference (LSD) at $P \leq 0.05$ was analyzed in the Statistical Analysis System-SAS (2018) program which was used to detect the effect of different factors on the studied parameters.

Results

Bacterial isolates

The results of this study revealed the isolation of *E. faecalis* from food samples (Fig. 2).

Iron oxide nanoparticles biosynthesis

Because no previous publications validate the use of *Enterococcus* to synthesize IONPs, the iron oxide nanoparticles were biosynthesized utilizing food origin *E. faecalis* for the first time globally. When the color begins to change from yellowish brown to brownish black, this will be the first insight into E-IONPs formation. Because iron oxide has a unique surface plasmon resonance feature, which causes the color change (Sundaram et al., 2012). UV–Vis's spectroscopy, AFM, and SEM were all used to figure out the iron oxide nanoparticles characteristics.

Characterizations of Enterococcus- Iron oxide nanoparticles

UV-Vis spectrum

When iron oxide nanoparticles were discovered in the reaction vessel throughout the incubation periods—which was the transformation of the reaction mixture from yellowish brown to brownish black—a UV-vis spectrophotometer was utilized to assess the biosynthesized E-IONPs. According to the results of this work, biosynthesized E-IONPs had a highest peak at 493 nm, as shown in Fig. 3. A common approach is UV-vis spectroscopy. The peaks were discovered to have a surface plasmon resonance spectroscopic signature produced by iron oxide nanoparticles (Mandal, 2018).

Fourier-transform infrared spectroscopy (FTIR)

The possible functional groups of biomolecules involved in the reduction and stabilization of biosynthesized E-IONPs were identified using FTIR. Stretching vibrations were discovered in the 400–4000 cm^{-1} range at 3425, 1750, 1416, 1091, 850, 455, and 590cm^{-1} by FT-IR analysis. Fe_3O_4-NPs have been synthesized by means of the reducing agent's presence in the sample. The presence of O–H stretching due to the presence of the OH-group is suggested by the peaks at 3425 cm^{-1}, which represent the alkane absorption peak. The C-H stretch of 1643 cm^{-1} represents the N-H bend absorption peak of amines, the 1568 cm^{-1} N-H bend of amides, the 1416cm^{-1} C=C stretch, and the 1091 cm^{-1} C-O stretch that represents the alcohol absorption peak. Ferrite low regions are indicated by peaks at 653 and 524 cm^{-1}, which could point to the formation of Fe_3O_4 NPs (Fig. 4).

Atomic force microscope (AFM)

To find out the E-IONPs average diameter and morphology in two and three dimensions, they were measured using atomic force microscopy as a confirmation tool for E-IONPs biosynthesis (Ajinkya et al., 2020). This study's result showed that the average size of E-IONPs was 48.77-55.55 nm, as shown in Table 2 and Fig. 5(a-c).

bioMérieux Customer:	Microbiology Chart Report	Printed October 9, 2021 2:47:21 AM CDT
Patient Name: Location: Lab ID: A		Patient ID: Physician: Isolate Number: 1
Organism Quantity: Selected Organism : Enterococcus faecalis Source: food		Collected:
Comments:		

Identification Information	Analysis Time:	2.92 hours	Status:	Final
Selected Organism	95% Probability Bionumber:	Enterococcus faecalis 154012711773461		
ID Analysis Messages				

Biochemical Details

2	AMY	+	4	PIPLC	-	5	dXYL	-	8	ADH1	+	9	BGAL	-	11	AGLU	+
13	APPA	-	14	CDEX	-	15	AspA	+	16	BGAR	-	17	AMAN	-	19	PHOS	-
20	LeuA	+	23	ProA	-	24	BGURr	-	25	AGAL	-	26	PyrA	+	27	BGUR	-
28	AlaA	+	29	TyrA	+	30	dSOR	+	31	URE	+	32	POLYB	-	37	dGAL	-
38	dRIB	+	39	ILATk	-	42	LAC	-	44	NAG	+	45	dMAL	+	46	BACI	+
47	NOVO	+	50	NC6.5	+	52	dMAN	+	53	dMNE	+	54	MBdG	+	56	PUL	-
57	dRAF	-	58	O129R	-	59	SAL	+	60	SAC	-	62	dTRE	+	63	ADH2s	+
64	OPTO	+															

Fig. 2. Report of Vitek assay clarify the identification of *E. faecalis*

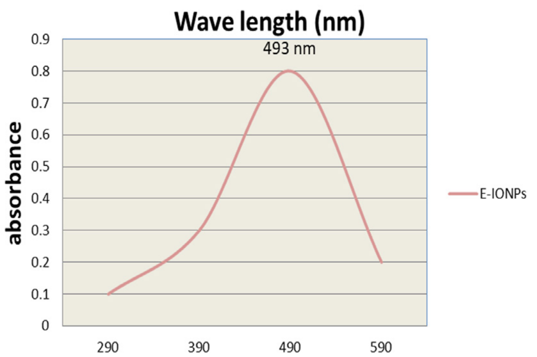

Fig. 3. The Uv-vis spectrophotometry of iron oxide nanoparticles biosynthesis by *E. faecalis*

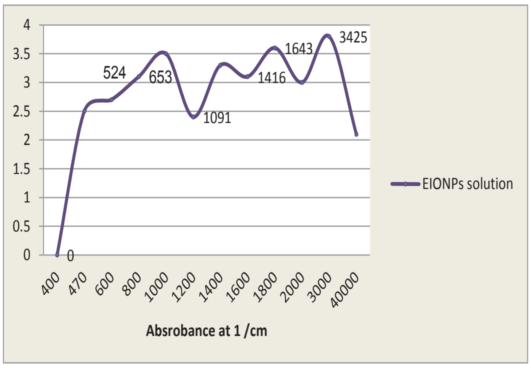

Fig. 4. FTIR analysis for iron oxide nanoparticles biosynthesized by *E. faecalis*

TABLE 2. Atomic force microscope measurements of the accumulation size of Iron oxide nanoparticles biosynthesized by food-origin *E. faecalis*

Avg. Diameter: 48.77 nm <=10% Diameter:20.00 nm

<=50% Diameter: 45.00 nmnm <=90% Diameter:75.00

Diameter (nm) <	Volume (%)	Cumulation (%)	Diameter (nm) <	Volume (%)	Cumulation (%)	Diameter (nm) <	Volume (%)	Cumulation (%)
10.00	0.31	0.31	70.00	6.74	75.99			
15.00	1.40	1.70	75.00	5.25	81.23	130.00	0.10	99.35
20.00	2.25	3.95	80.00	4.87	86.10	135.00	0.17	99.52
25.00	3.61	7.56	85.00	3.47	89.58	140.00	0.10	99.63
30.00	4.39	11.96	90.00	3.03	92.61	145.00	0.03	99.66
35.00	7.49	19.45	95.00	2.04	94.65	150.00	0.10	99.76
40.00	7.05	26.50	100.00	1.43	96.08	155.00	0.07	99.83
45.00	9.23	35.73	105.00	0.99	97.07	180.00	0.03	99.86
50.00	9.57	45.30	110.00	0.61	97.68	185.00	0.07	99.93
55.00	7.39	52.69	115.00	0.75	98.43	195.00	0.03	99.97
60.00	9.06	61.75	120.00	0.34	98.77	200.00	0.03	100.00
65.00	7.49	69.24	125.00	0.48	99.25			

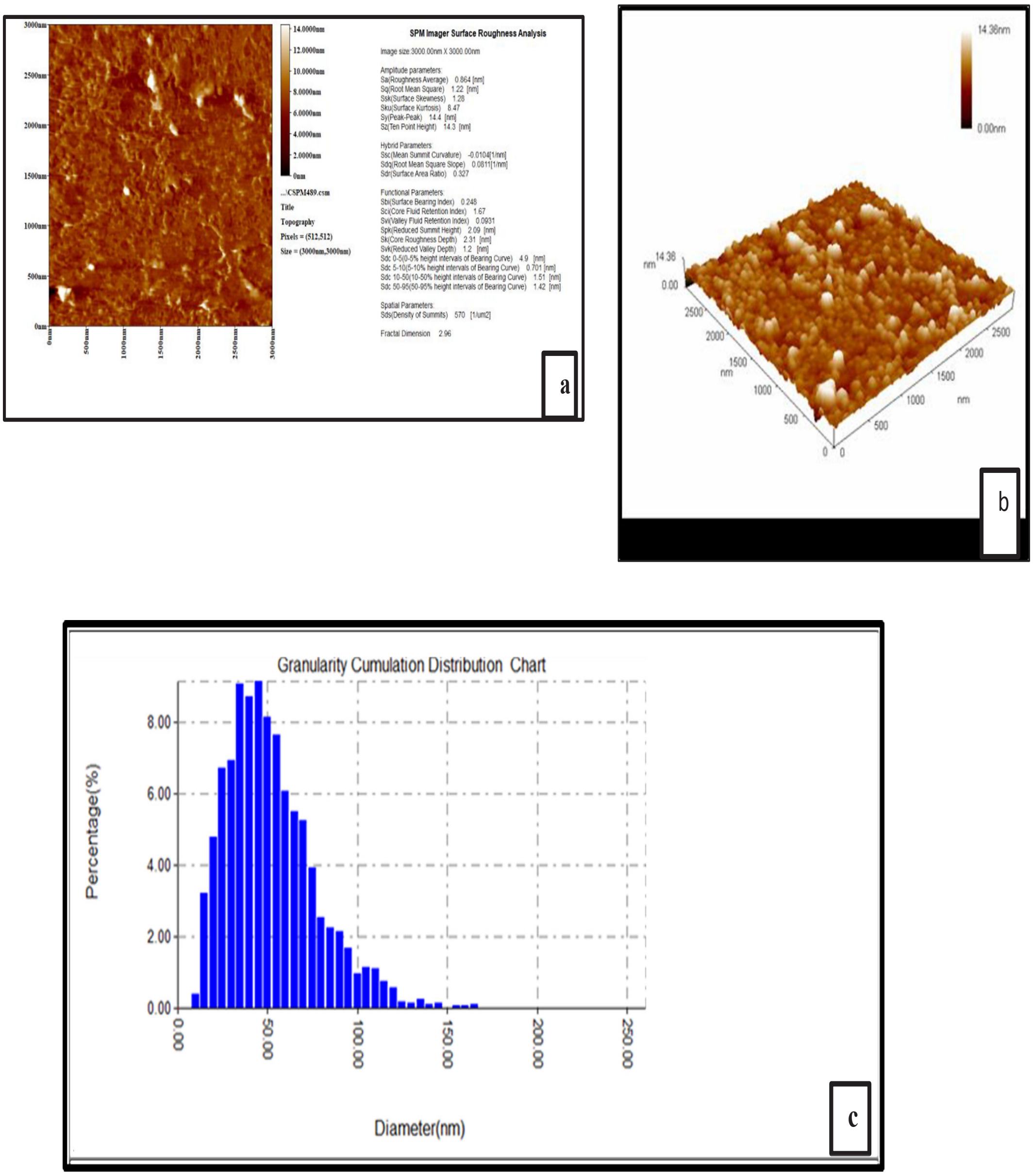

Fig. 5. Biosynthesis E-IONPs by *E. faecalis* under AFM (a), 2D image of iron oxide nanoparticles synthesis (b), 3D image of iron nanoparticles synthesis and (c) granularity distribution chart of iron oxide nanoparticles synthesized

Scanning electron microscope (SEM)

Following color change, UV-vis spectroscopy, FTIR, and AFM investigations, the SEM was used to determine the predictable shape of the biosynthesized E-IONPs (Arjaghi et al., 2021). EIONPs biosynthesis was confirmed by the results. Cubic shape E-IONPs were detected as shown in Fig. 6.

Determination of the optimum conditions for E-IONPs biosynthesis

The optimum conditions for the biosynthesis of super-magnatic iron oxide were: 3:1 addition mixture of reaction; 3mL of *E. faecalis* bacteria supernatant to 1mL of iron oxide solution that is at 1M of concentration at 60°C for incubation period of 24h at pH of 5.

Evaluation of antibiofilm activity of Iron oxide nanoparticle

According to the results of E-IONPs antibiofilm activity conducted in this work, the treatment of 2mg mL^{-1} of E-IONPs showed 44% biofilm reduction for *E. coli* (A), 45% for *S. aureus* (B), 46% for *K. pneumoniae* (C) and 44% for *S. agalactiae* (D). The results of biofilm reduction of 44% which mean no significant biofilm reduction, at 3mg mL^{-1} showed 50, 65, 63, and 50%, respectively, for bacterial isolates that were considered significant biofilm reduction (P≤0.05), while at 4mg mL^{-1} that showed a highly significant (P≤0.01) reduction then exhibited 75 (A), 81 (B), 74 (C), and 75% (D), respectively. (Tables 3 and 4, Fig. 7).

TABLE 3. **Statistical results of the effect of E-IONPs against *E. coli* (A), *S. aureus* (B), *K. pneumoniae* (C), and *S. agalactiae* (D) biofilms**

Bacterial isolate	A	B	C	D	C1	C2
Before treatment By EIONPs	0.178	0.240	0.184	0.165	0.041	0.104
After treatment By E-IONPs (mg/mL)						
2	0.101	0.132	0.119	0.110	0.044	0.044
3	0.090	0.085	0.088	0.084	0.044	0.044
4	0.045	0.046	0.049	0.042	0.044	0.044
P-value	0.0094 **	0.0012 **	0.0087 **	0.0076 **	0.923 NS	0.041 *

* (P≤0.05) ** (P≤0.01), NS: Non-Significant.

Control-1(C1): Just broth medium as a negative control, control-2(C2): broth plus E-IONPs as a negative control, and positive control (+Ve): inoculated broth without treatment.

TABLE 4. The percentages of biofilm reduction of clinical bacterial isolates after treatment with concentrations (2, 3, and 4 mg mL^{-1}) of EIONPs

E-IONPs concentration (mg mL^{-1})	*E. coli*	*S. aureus*	*K. pneumoniae*	*S. agalactiae*
2	44%	45%	46%	44%
3	50%,	65%	63%	50%
4	75%	81%	74%	75%

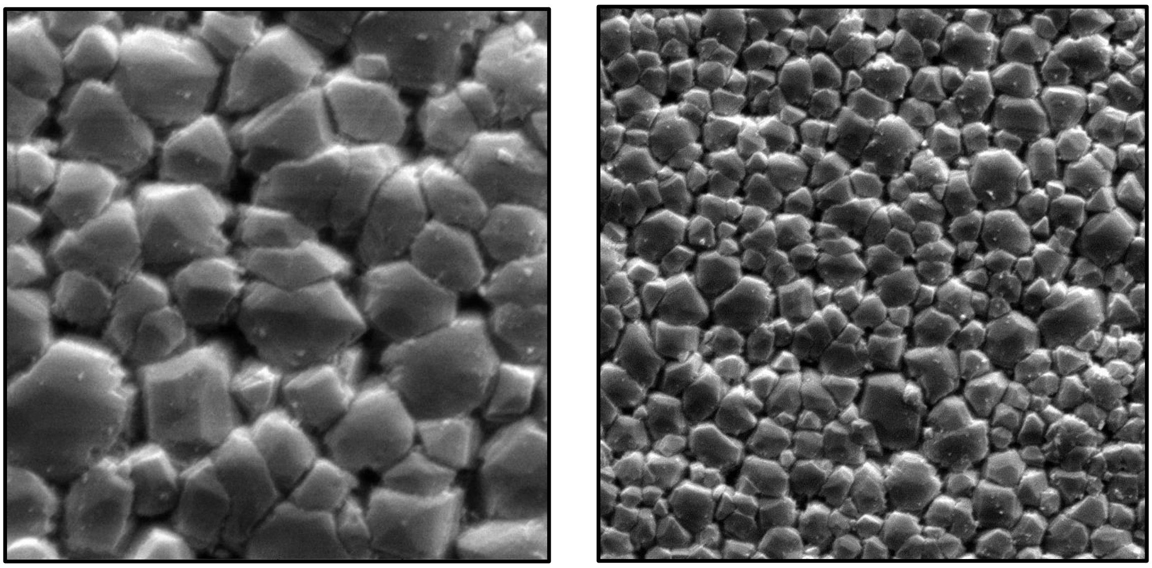

Fig. 6. Biosynthesized Iron oxide NPs by food origin *E. faecalis* under SEM as detected with cubical shape

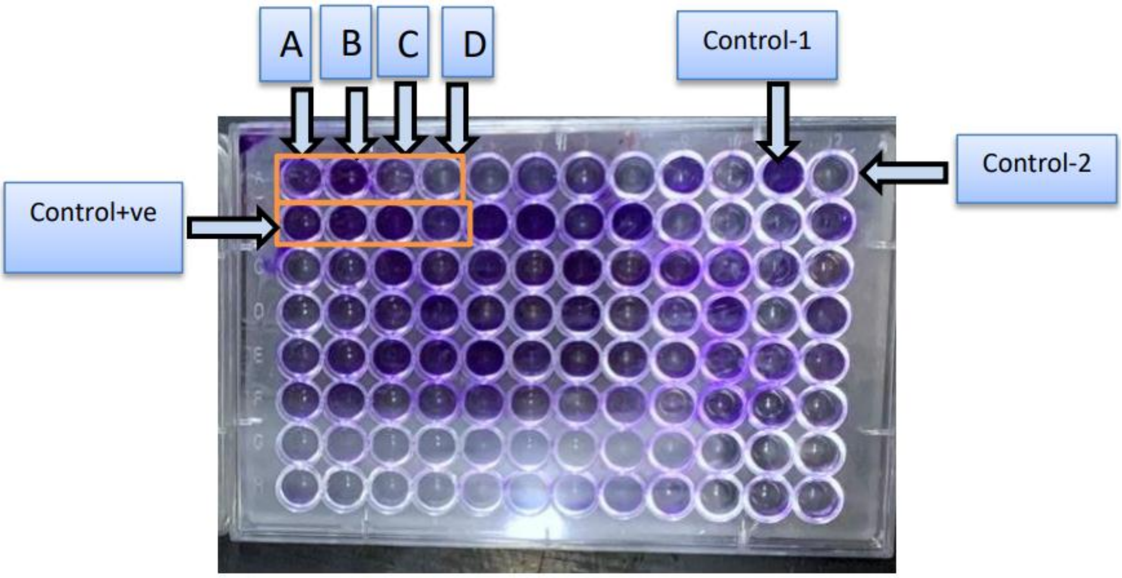

Fig. 7. Microtitter plate after crystal violet stain to diagnostic impact of E-IONPs against biofilm formed by A, B, C and D isolates [control+ve: after treating by E-IONPs at 4mg/mL, control-1: only nutrient broth, control-2: N.B+E-IONPs]

Discussion

Treatment of biofilm-associated infections has a substantial challenge since bacteria can become resistant to standard antimicrobial agents. To address the issue of recurring infections caused by biofilms, this study looked for alternatives to antibiotics. The super-magnetic iron oxide NPs produced by biosynthesis stand in for this alternative medication. Food origin *E. faecalis* was used as a safe and eco-friendly method to synthesize E-IONPs (Álvarez et al., 2022).

Food samples were utilized to isolate *E. faecalis* that is employed as a reducing agent in the production of E-IONPs (vegetables and meat). In Korea, *E. faecalis* was isolated from food of an animal origin, according to Kim et al. (2021). This bacterium was isolated from white cheeses from Turkey and Iran, according to a different investigation (Oruc et al., 2021).

When there is a colour shift, that is the first sign that E-IONPs are forming (Sandhya & Kalaiselvam, 2020). After the pH was tuned, the reaction mixture's hue changed from yellowish brown to light yellow, then to black, and this outcome matched Kaur & Chopra's findings (2018). Additionally, Selah & Mohammad's research from the year 2021 revealed that the colour of the resultant substance changed from yellow to brown following 24h of incubation and from brown to black after two days of incubation (Selah & Mohammad, 2021).

In this investigation, UV peaks at 493 nm in the visible portion of the UV-spectrum served as confirmation for the creation of E-IONPs. For biosynthetic IONPs, UV-vis revealed a distinctive surface plasmon resonance peak (Hammad et al., 2022). The achieved peak in this investigation agreed with the findings of Thenmozhi et al. (2019). IONPs were found at 658nm in UV spectra in Kanagasubbulakshmi & Kadirvelu's (2017) study employing plant based IONPs synthesis.

To identify the effective groups in a very particular manner, the Fourier transform infrared examination was used. The findings of studies conducted in (2016) by Pham et al. and in (2021) by Majeed et al. were comparable to those of our investigation. IONPs were created utilizing bacteria, and FTIR spectra analysis was used to determine the chemical composition and functional group, which might operate as a capping agent to assist stabilized nanoparticles by perhaps reducing Fe ions or possibly interacting with NPs (Al-Maliki & Taj-Aldeen, 2021). The iron oxide NPs green manufacturing technique by Devi et al. (2019) detected FeNPs stretching vibrations at 663, 462, and 426cm^{-1}. The production of NPs at 694cm^{-1} strength was validated by a second publication on the green synthesis of IONPs (Abid & Kadhim, 2022). In contrast, IONPs synthesized chemically using a process that produced IONPs maghemite as evidenced by FTIR data in the bands 526.75 and 690.61cm^{-1} (Shin et al., 2019).

Atomic force microscope analysis was used to determine the size of IONPs (Takai et al., 2019). According to the AFM data of this research, most of the particles were cubes within the size range 48.77-55.55nm. The average diameter percentage of nanoparticles present also in the study of Behera et al. (2012) which was around 66nm. On the other hand, IONPs that were chemically synthesized were in size range of 14.53 to 20.54nm (Samrot et al., 2020). Particles were found to be spherical in shape, mono-dispersed, and with a diameter of less than 50nm (Kaur & Chopra, 2018). The report by Pieretti et al. (2020) used a green synthesis method to form Fe_3O_4 NPs hybrid with AgNPs with an average diameter size of 25nm. IONPs (Fe_2O_3) were in size ranges from 3-46nm that chemically synthesized with the aid of sol-gel method (Khan et al., 2021). Using $FeSo_4.7H_2O$ as a substrate for biosynthesis of Fe_2O_3 NPs that were at a range of 60 -80nm *via* fungi as a reducing agent (Saied et al., 2022). Study by Housseiny & Gomaa (2019) obtained spherical monodispersed Zinc nanoparticles from 9 to 17nm in average diameter by biologically method.

To determine the morphology of E-IONPs, SEM was performed. This work's SEM imaging revealed that the E-IONPs were cubic in form (nano cubes). Iron oxide cubic nanoparticles were also reported by Sayed & Polshettiwar (2015). Meanwhile, the outcomes of the green approach used by Kirdat et al. (2021) to synthesis IONPs. When examined under a SEM, the IONPs produced by Saqib et al. (2019) were spherical (25-40nm). A portion of the antibiofilm activity of iron oxide nanoparticles (IONPs) can be attributed to their unique magnetic characteristics, which can be utilized in a range of medicinal applications. Biofilms are mechanically impacted by IONPs when an external magnet is present (Velusamy et al., 2022). In the results of this research, E-IONPs at a low concentration (1mg mL^{-1}) appear insignificant in the biofilm reduction, while at a concentration of 4 mg mL^{-1} showed a highly significant ($P \leq 0.01$) inhibition of *K. pneumoniae*, *E. coli, S. agalactiae,* and *S. aureus* biofilms. The resulted of the anti-biofilm effect is well agreed with recent research that used the green synthesized chitosan-coated IONPs at 4mg mL^{-1} and showed a significant reduction of biofilm formed by *S. aureus* (Mohaidin et al., 2022). Another study by Subhi (2018) used 50mg mL^{-1} of chitosan-coated IONPs for inhibition of bacterial biofilm of *E. coli* and *S. aureus* clinical isolates and the results showed a highly significant reduction ($P>0.05$) in the biofilm that formed while in obtained data by Rasul et al. (2020). The MIC were 75mg mL^{-1} of IONPs as an antibiofilm against *S. agalactiae* that the Iron oxide nanoparticles lead to a reduction of 74.13% in the biofilm formation. The most well-known studies in the field of IONPs employed against planktonic *K. pneumoniae* in Ansari et al. (2017), whereas testing the antibiofilm efficacy of the E-IONPs against biofilms generated by aggressive bacterial species like *K. pneumoniae* was not preceded by any prior studies. According to Salari et al. (2018) and Abdul et al. (2019), there is a correlation between the concentration of IONPs and the biofilm thinning; in other words, the higher the IONPs concentration, the greater the percentage of biofilm that has been decreased.

Treatment with iron oxide nanoparticles at a concentration of 4mg mL^{-1} totally (about 90%) prevented the growth of biofilm. Additionally, the information gathered showed that biologically produced iron oxide nanoparticles (E-IONPs) at a concentration of 4mg mL^{-1} not only successfully suppressed bacterial growth but were also linked to the suppression of the biofilm that had developed. E-IONPs have an inhibitory impact when they break through an impermeable barrier (Extracellular Polysaccharide) that most antibiotics form, rupturing cell membranes and hindering the development of biofilm (Velusamy et al., 2022). The nano-scale diameter of the metal particles, which results in a higher surface area-to-volume ratio, is one of the many benefits of the metal's transformation into nanoparticles.

Given their distinct physiochemical properties, nanoparticles are thought to have their antibacterial action because of their high ratio (Masadeh et al., 2015). The efficiency of iron oxide nanoparticles was hypothesized to be due more to their high surface-to-volume ratio than to the single action of the release of metal ions (Noqta et al., 2019). In conjunction with the increased surface-volume ratio, reactive oxygen radicles are formed in considerable quantities (Li et al., 2021). Multiple researches suggested Silver nanoparticles'mode of action involves adhering to the surface of the cell membrane and interfering with the permeability and respiration processes (Mohy El-Din & El Said, 2017). Our results recommended that: Studying the ability of the other species of *Enterococcus* for nanoparticles biosynthesis, studying the antifungal and anticancer activity of nanoparticles that biosynthesized by food-origin *Enterococcus* spp. *in vitro* and *in vivo*, and studying the ability of food origin *E. faecails* for the biosynthesis of other types of nanometals and nanodrugs.

Conclusions

The utilization of the food-origin bacterial isolate *E. faecalis* to make iron oxide nanoparticles in a simple, inexpensive, and environmentally acceptable way is the work's main restriction. This biosynthesis was performed under the ideal circumstances. Super-magnetic E-IONPs with cubic shapes that range in size from 48.77 to 55.55 nm were biosynthesized. In addition to planktonic bacterial isolates of Gram positive and Gram-negative species, such as *E. coli*, *S. aureus*, *K. pneumoniae*, and *S. agalactiae*, super-magnetic E-IONPs which could inhibit bacteria that form biofilms.

Competing interests: The authors report no conflicts of interest regarding this work.

Authors' contributions: Conceptualization, methodology, validation, investigation, resources, writing original draft preparation, writing review and editing, M.A.A and M.H.A.

Ethics approval: Not applicable.

Reference

Abdul, F.R., Subhi, H.T., Taher, N.A., Raheem, I.A. (2019) Activity of Iron oxide nanoparticles on bacterial biofilm formation. *Journal of Pharmaceutical Sciences and Research*, **11**(3), 1126-1130.

Abid, M.A., Kadhim, D.A. (2022) Synthesis of iron oxide nanoparticles by mixing chilli with rust iron extract to examine antibacterial activity. *Materials Technology,* **37**(10), 1494-1503.

Ajinkya, N., Yu, X., Kaithal, P., Luo, H., Somani, P., Ramakrishna, S. (2020) Magnetic iron oxide nanoparticle (IONP) synthesis to applications: present and future. *Materials*, **13**(20), 4644.

Al-Maliki, Q.A., Taj-Aldeen, W.R. (2021) Antibacterial and antibiofilm activity of bacteria mediated synthesized Fe_3O_4 nanoparticles Using *Bacillus coagulans*. *Journal of Nanostructures,* **11**(4), 782-789.

Álvarez, E., Estévez, M., Gallo-Cordova, A., González, B., Castillo, R.R., Morales, M.D.P., Vallet-Regí, M. (2022) Superparamagnetic iron oxide nanoparticles decorated mesoporous silica nanosystem for combined antibiofilm therapy. *Pharmaceutics*, **14**(1), 163.

Ansari, S.A., Oves, M., Satar, R., Khan, A., Ahmad, S.I., Jafri, M.A., Algahtani, M.H. (2017) Antibacterial activity of iron oxide nanoparticles synthesized by co-precipitation technology against *Bacillus cereus* and *Klebsiella pneumoniae*. *Polish Journal of Chemical Technology*, **19**(4), 110—115.

Arjaghi, S.K., Alasl, M.K., Sajjadi, N., Fataei, E., Rajaei, G.E. (2021) Retracted article: green synthesis of Iron oxide nanoparticles by RS Lichen extract and its application in removing heavy metals of lead and cadmium. *Biological Trace Element Research*, **199**(2), 763-768.

Behera, S.S., Patra, J.K., Pramanik, K., Panda, N., Thatoi, H. (2012) Characterization and evaluation of antibacterial activities of chemically synthesized iron oxide nanoparticles, World Journal of Nano Science and Engineering, **2**, 196-200.

Benson, T. (2001) "*Microbiological Applications Laboratory Manual in General Microbiology*". 8th ed., the McGraw-Hill, New York.

Devi, H.S., Boda, M.A., Shah, M.A., Parveen, S., Wani, A.H. (2019) Green synthesis of iron oxide nanoparticles using *Platanus orientalis* leaf extract for antifungal activity. *Green Processing and Synthesis*, **8**(1), 38-45.

Galindo-Méndez, M. (2020) Antimicrobial resistance in *Escherichia coli*. In: " *E. coli Infections - Importance of Early Diagnosis and Efficient Treatment*". IntechOpen. https://doi.org/10.5772/intechopen.93115

Grassi, P., Reis, C., Drumm, F.C., Georgin, J., Tonato, D., Escudero, L.B., Dotto, G.L. (2019) Biosorption of crystal violet dye using inactive biomass of the fungus Diaporthe schini. *Water Science and Technology*, **79**(4), 709-717.

Hammad, E.N., Salem, S.S., Mohamed, A.A., El-Dougdoug, W. (2022) Environmental impacts of ecofriendly Iron oxide nanoparticles on dyes removal and antibacterial activity. *Applied Biochemistry and Biotechnology*, https://doi.org/10.1007/s12010-022-04105-1.

Hashim, M.H., AlKhafaji, M.H. (2018) Isolation and identification of *Citrobacter freundii* from chicken meat samples using cultural and molecular techniques. *Iraqi Journal of Science*, **59**(3A), 1216-1224.

Hassan, D.F., Mahmood, M.B. (2019) Biosynthesis of iron oxide nanoparticles using *Escherichia coli. Iraqi Journal of Science*, **60**(3), 453-459.

Housseiny, M.M., Gomaa, E.Z. (2019) Enhancement of antimicrobial and antitumor activities of zinc nanoparticles biosynthesized by *Penicillium chrysogenum* AUMC 10608 using gamma radiation. *Egyptian Journal of Botany*, **59**(2), 319-337.

Huh, A.J., Kwon, Y.J. (2011) ''Nanoantibiotics'': a new paradigm for treating infectious diseases using nanomaterials in the antibiotics resistant era. *Journal of Controlled Release*, **156**, 128–145.

Jogi, A.R., Bordoloi, S., Himani, K., Lade, A., Sehar, R. (2022) Phenotypic detection and comparison of biofilm production in methicillin resistant *Staphylococcus aureus*. *The Pharma Innovation Journal,* **SP-11**(3), 1352-1357.

Kanagasubbulakshmi, S., Kadirvelu, K. (2017) Green synthesis of iron oxide nanoparticles using *Lagenaria siceraria* and evaluation of its antimicrobial activity. *Defense Life Science Journal,* **2**(4), 422-427.

Kaur, M., Chopra, D.S. (2018) Green synthesis of iron nanoparticles for biomedical applications. *Global Journal of Nanomedicine*, **4**(4), 68-76.

Khan, I., Morishita, S., Higashinaka, R., Matsuda, T. D., Aoki, Y., Kuzmann, E., Kubuki, S. (2021) Synthesis, characterization and magnetic properties of ε-Fe_2O_3 nanoparticles prepared by sol-gel method. *Journal of Magnetism and Magnetic Materials*, **538**, 168264.

Kim, E., Shin, S.W., Kwak, H.S., Cha, M.H., Yang, S.M., Gwak, Y.S., Kim, H.Y. (2021) Prevalence and characteristics of phenicol-oxazolidinone resistance genes in Enterococcus faecalis and *Enterococcus faecium* isolated from food-producing animals and meat in Korea. *International Journal of Molecular Sciences,* **22**(21), 11335.

Kirdat, P.N., Dandge, P.B., Hagwane, R.M., Nikam, A.S., Mahadik, S.P., Jirange, S.T. (2021) Synthesis and characterization of ginger (*Z. officinale*) extract mediated iron oxide nanoparticles and its antibacterial activity. *Materials Today: Proceedings*, **43**, 2826-2831.

Kumar Shrestha, B., Tumbahangphe, M., Shakya, J., Chauhan, S. (2022) Uropathogenic *Escherichia coli* in urinary tract infections: A review on epidemiology, pathogenesis, clinical manifestation, diagnosis, treatments and prevention. *Novel Research in Microbiology Journal,* **6**(4), 1614-1634.

Larsen, J., Raisen, C.L., Ba, X., Sadgrove, N.J., Padilla-González, G.F., Simmonds, M.S., Larsen, A.R. (2022) Emergence of methicillin resistance predates the clinical use of antibiotics. *Nature*, **602**(7895), 135-141.

Li, Y., Yang, J., Sun, X. (2021) Reactive oxygen species-based nanomaterials for cancer therapy. *Frontiers in Chemistry*, **9**, 650587.

Majeed, S., Danish, M., Mohamad Ibrahim, M.N., Sekeri, S. H., Ansari, M.T., Nanda, A., Ahmad, G. (2021) Bacteria mediated synthesis of iron oxide nanoparticles and their antibacterial, antioxidant, cytocompatibility properties. *Journal of Cluster Science,* **32**(4), 1083-1094.

Manandhar, S., Singh, A., Varma, A., Pandey, S., Shrivastava, N. (2018) Evaluation of methods to detect in *vitro* biofilm formation by staphylococcal clinical isolates. *BMC Research Notes*, **11**(1), 1-6.

Mandal, A.K. (2018) Mesoporous silica nanoparticles as delivery system against diseases. *Methods*, **27**, 32.

Mao, Q., Sun, X., Sun, J., Zhang, F., Lv, A., Hu, X., Guo, Y. (2020) A candidate probiotic strain of Enterococcus faecium from the intestine of the crucian carp *Carassius auratus*. *AMB Express,* **10**(1), 1-9.

Masadeh, M.M., Karasneh, G.A., Al-Akhras, M.A., Albiss, B.A., Aljarah, K.M., Al-Azzam, S.I., Alzoubi, K.H., (2015) Cerium oxide and iron oxide nanoparticles abolish the antibacterial activity of ciprofloxacin against gram positive and gram negative biofilm bacteria. *Cytotechnology,* **67**(3), 427-435.

Mba, I.E., Nweze, E.I. (2021) Nanoparticles as therapeutic options for treating multidrug-resistant bacteria: Research progress, challenges, and prospects. *World Journal of Microbiology and Biotechnology*, **37**(6), 1-30.

Mohaidin, N.L.M., Aris, F., Amin, I.M., Zain, N.M., Yunus, N.M., Izza, N. (2022) Antibiofilm property of green synthesized iron oxide nanoparticles from neem leaves. *Journal of Sustainability Science and Management*, **17**(3), 279-290.

Mohy El-Din, S.M., El Said, H.S. (2017) Biosynthesis of silver nanoparticles from the marine microalga *Isochrysis galbana* and their antibacterial activity against pathogenic bacteria. *Egyptian Journal of Botany*, **56**(2), 371-379.

Nadeem, M., Khan, R., Shah, N., Bangash, I. R., Abbasi, B. H., Hano, C., Celli, J. (2021) A review of microbial mediated iron nanoparticles (IONPs) and its biomedical applications. *Nanomaterials*, **12**(1), 130.

Nixon, W. (2008) The general principles of scanning electron microscopy. Philosophical Transactions of the Royal Society of London. *Series B. Biological Sciences*, **261**(837), 45-50.

Noqta, O.A., Aziz, A.A., Usman, I.A., Bououdina, M. (2019) Recent advances in iron oxide nanoparticles (IONPs): synthesis and surface modification for biomedical applications. *Journal of Superconductivity and Novel Magnetism,* **32**(4), 779-795.

Odoki, M., Almustapha Aliero, A., Tibyangye, J., Nyabayo Maniga, J., Wampande, E., Drago Kato, C., Bazira, J., (2019) Prevalence of bacterial urinary tract infections and associated factors among patients attending hospitals in Bushenyi district, Uganda. *International Journal of Microbiology*, https://doi.org/10.1155/2019/4246780.

Ojo, O.A., Olayide, I.I., Akalabu, M.C., Ajiboye, B.O., Ojo, A.B., Oyinloye, B.E., Ramalingam, M. (2021) Nanoparticles and their biomedical applications. *Biointerface Research in Applied Chemistry*, **11**(1), 8431-8445.

Oruc, O., Cetin, O., Darilmaz, D.O., Yüsekdag, Z.N. (2021) Determination of the biosafety of potential probiotic *Enterococcus faecalis* and *Enterococcus faecium* strains isolated from traditional white cheeses. *Lebensmittel-Wissenschaft & Technologie,* **148**, 111741.

Paudel, D., Regmi, H., Bajracharya, U., Shrestha, G.K. (2021) Spectrum and presentation of urinary bladder growth: a single-center retrospective study. *Nepalese Medical Journal*, **4**(2), 485-488.

Pham, X., Nguyen T., Phuoc, Pham, T., Tran, Thi, Tran, T. (2016) Synthesis and characterization of chitosan-coated magnetite nanoparticles and their application in curcumin drug delivery. *Advances in Natural Sciences: Nanoscience and Nanotechnology*. **7**. 045010. 10.1088/2043-6262/7/4/045010.

Pieretti, J.C., Rolim, W.R., Ferreira, F.F., Lombello, C.B., Nascimento, M.H., Seabra, A.B. (2020) Synthesis, characterization, and cytotoxicity of Fe_3O_4@ Ag hybrid nanoparticles: promising applications in cancer treatment. *Journal of Cluster Science*, **31**(2), 535-547.

Priya, B.B. (2019) A review on urinary tract infection. *World Journal of Pharmaceutical Research*, **9**(1), 602-625.

Rasul, S.O.T., Mustafa, K.K., Abdulrahman, Z.F.A. (2020) Iron oxide nanoparticles reduced biofilm formation and detection of lmb genes in *Streptococcus agalactiae* isolated from patients with Diabetes Mellitus. *Medico-legal Update*, **20**(1), 347.

Saied, E., Salem, S.S., Al-Askar, A.A., Elkady, F.M., Arishi, A.A., Hashem, A.H. (2022) Mycosynthesis of hematite (α-Fe_2O_3) nanoparticles using *Aspergillus niger* and their antimicrobial and photocatalytic activities. *Bioengineering*, **9**(8), 397.

Salari, S., Seddighi, N.S., Almani, P.G.N. (2018) Evaluation of biofilm formation ability in different Candida strains and anti-biofilm effects of Fe_3O_4-NPs compared with Fluconazole: an in vitro study. *Journal de Mycologie Medicale,* **28**(1), 23-28.

Sampora, Y., Hardiansyah, A., Khaerudini, D.S., Burhani, D., Sondari, D., Septiyanti, M., Septevani, A.A. (2022) Synthesis and characterization of magnetite nanoparticle for removal of heavy metal ions from aqueous solutions. *In IOP Conference Series: Earth and Environmental Science* (Vol. 1017, No. 1, p. 012017). IOP Publishing.

Samrot, A.V., SaiPriya, C., Selvarani, J., PJ, J.C., Lavanya, Y., Soundarya, P., Varghese, R.J. (2020) A study on influence of superparamagnetic iron oxide nanoparticles (SPIONs) on green gram (*Vigna radiata* L.) and earthworm (*Eudrilus eugeniae* L.). *Materials Research Express*, **7**(5), 055002.

Sandhya, J., Kalaiselvam, S. (2020) Biogenic synthesis of magnetic iron oxide nanoparticles using inedible borassus flabellifer seed coat: characterization, antimicrobial, antioxidant activity and in vitro cytotoxicity analysis. *Materials Research Express,* **7**(1), 015045.

Saqib, S., Munis, M.F.H., Zaman, W., Ullah, F., Shah, S.N., Ayaz, A., Bahadur, S. (2019) Synthesis, characterization and use of iron oxide nano particles for antibacterial activity. *Microscopy Research and Technique,* **82**(4), 415-420.

Sayed, F.N., Polshettiwar, V. (2015) Facile and sustainable synthesis of shaped iron oxide nanoparticles: effect of iron precursor salts on the shapes of iron oxides. *Scientific Reports*, **5**(1), 1-14.

SAS (2018) "*Statistical Analysis System, User's Guide*". Statistical. Version 9.6th ed. SAS. Inst. Inc. Cary. N.C. USA.

Selah, M.T., Mohammad, G.A. (2021) Ability of three species of enterobacter bacteria to synthesize iron nanoparticles and detection of the efficacy to inhibitory effect on other pathogenic bacteria. *Biochemical and Cellular Archives*, **21** (Suppl 1), 2085-2090.

Shi, X., Qing, W., Marhaba, T., Zhang, W. (2020) Atomic force microscopy-Scanning electrochemical microscopy (AFM-SECM) for nanoscale topographical and electrochemical characterization: Principles, applications and perspectives. *Electrochimica Acta*, **332**, 135472.

Shin, N., Saravanakumar, K., Wang, M.H. (2019) Sonochemical mediated synthesis of iron oxide (Fe_3O_4 and Fe_2O_3) nanoparticles and their characterization, cytotoxicity and antibacterial properties. *Journal of Cluster Science,* **30**(3), 669-675.

Shkodenko, L., Kassirov, I., Koshel, E. (2020) Metal oxide nanoparticles against bacterial biofilms: perspectives and limitations. *Microorganisms*, **8**(10), 1545.

Singh, S., Datta, S., Narayanan, K.B., Rajnish, K.N. (2021) Bacterial exo-polysaccharides in biofilms: role in antimicrobial resistance and treatments. *Journal of Genetic Engineering and Biotechnology,* **19**(1), 1-19.

Sohal, J.K., Saraf, A., Shukla, K.K. (2021) Silver nanoparticles (AgNPs): methods of synthesis, mechanism of antimicrobial action and applications. "*Multidisciplinary Research and Development*", pp. 55-71.

Subhi, H.T. (2018) Activity of iron oxide nanoparticles-chitosan composite on bacterial biofilm formation. *In Proceedings of the 2018 International Conference on Pure and Applied Sciences.*

Sundaram, P.A., Augustine, R., Kannan, M. (2012) Extracellular biosynthesis of iron oxide nanoparticles by Bacillus subtilis strains isolated from rhizosphere soil. *Biotechnology and Bioprocess Engineering,* **17**(4), 835-840.

Swan, A. (1954) The use of a bile-aesculin medium and of Maxted's technique of Lancefield grouping in the identification of enterococci (group D streptococci). *Journal of Clinical Pathology,* **7**(2), 160–163.

Takai, Z.I., Mustafa, M.K., Asman, S., Sekak, K.A. (2019) Preparation and characterization of magnetite (Fe_3O_4) nanoparticles by sol-gel method. *International Journal of Nanoelectronics*, **12**, 37-46.

Thenmozhi, T, Nadella, Rasajna, Megala, Rajesh, Nannepaga, John S. (2019) Biosynthesis and characterization of iron oxide nanoparticles via *Syzygium aromaticum* extract and determination of its cytotoxicity against human breast cancer cell lines. 5. 587-592. 10.30799/jnst.178.19050103.

Üstün, E., Önbaş, S.C., Çelik, S.K., Ayvaz, M.Ç., Şahin, N. (2022) Green synthesis of iron oxide nanoparticles by using *Ficus carica* leaf extract and its antioxidant activity. *Biointerface Research in Applied Chemistry*, **12**(2), 2108-2116.

Velusamy, P., Su, C.H., Kannan, K., Kumar, G.V., Anbu, P., Gopinath, S.C. (2022) Surface engineered iron oxide nanoparticles as efficient materials for antibiofilm application. *Biotechnology and Applied Biochemistry*, **69**(2), 714-725.

Wu, D., Ding, Y., Yao, K., Gao, W., Wang, Y. (2021) Antimicrobial resistance analysis of clinical *Escherichia coli* isolates in neonatal ward. *Frontiers in Pediatrics*, **9**, 670470.

Yazdanian, M., Rostamzadeh, P., Rahbar, M., Alam, M., Abbasi, K., Tahmasebi, E., Yazdanian, A. (2022) The potential application of green-synthesized metal nanoparticles in dentistry: A comprehensive review. *Bioinorganic Chemistry and Applications*. https://doi.org/10.1155/2022/2311910

Yerlikaya, O., Akbulut, N. (2020) Identification, biochemical and technological properties of *Enterococcus* species isolated from raw milk and traditional dairy products. *Ukrainian Food Journal*, **9**(4), 809-934.

Youssef, G.A., El-Boraey, A.M., Abdel-Tawab, M.M. (2019) Eco-friendly green synthesis of silver nanoparticles from egyptian honey: Evaluating its antibacterial activities. *Egyptian Journal of Botany,* **59**(3), 709-721.

الفاعلية المضادة للغشاء الحياتي لدقائق الحديد النانوية المصنعة حيويا من المكورات المعوية ضد البكتريا الممرضة البولية

محمد احمد علي، مروى حميد الخفاجي
قسم علوم الحياة- كلية العلوم- جامعة بغداد- بغداد- العراق.

تلعب عوامل الفوعة مثل الغشاء الحياتي دورًا مهمًا في إمراضية البكتيريا. يصيب مرض التهابات المسالك البولية ملايين الأشخاص حول العالم يتسبب بفعل البكتريا عالية المقاومة لمضادات الميكروبات. لذلك هدفت هذه الدراسة إلى إيجاد حل لهذه المشكلة العالمية باستخدام الدقائق النانوية كمضادات جرثومية حديثة. تم تصنيع دقائق أوكسيد الحديد النانوية (E-IONPs) حيوياً باستخدام عزلات *Enterococcus faecalis* ذات الأصل الغذائي لأول مرة عالميا. تم إجراء عملية التصنيع الحيوي في ظروف مثلى: من محلول الحديد بتركيز 1 مولاري بدرجة 60 مئوية بعد فترة حضانة 24 ساعة في دالة حامضية بقيمة 5. تم عزل العزلات البكتيرية من العينات السريرية والغذائية. وبعد تشخيصها، تم استخدام بكتيريا الأصل الغذائي في عملية التصنيع الحيوي، في حين تم اختبار العزلات السريرية لقدرتها على تكوين الغشاء الحياتي. تم تشخيص E-IONPs المصنعة حيوياً أولاً عن طريق تغيير اللون، ثم عن طريق التحليل الطيفي للأشعة فوق البنفسجية، وتحليل مجهر القوة الذرية، وتحليل FTIR والمجهر الالكتروني الماسح. تم اختبار النشاط المضاد للغشاء الحياتي لـ E-IONPs فائقة المغناطيسية باستخدام اختبار اطباق المعايرة الدقيقة. أوضحت النتائج التي تم الحصول عليها من هذه الدراسة أنE-IONPs المصنعة حيوياً كانت مكعبة وغير منتظمة الشكل ضمن نطاق حجم 48.77-55.55 نانومتر، ولها نشاط مضاد للغشاء الحياتي. في الختام: كانت الدقائق النانوية لأوكسيد الحديد فائقة المغناطيسية المُصنَّعة حيوياً فعالة ضد الأغشية الحيوية التي تكونت بواسطة البكتيريا الممرضة البولية.